IRAMP
2(2), Dec. 2011, pp. 93-98

ISSN: 2229-3159

Spectral Lines of Multi-Charged Fluorine from a Plasma Interacting with a Strong Quasimonochromatic Electric Field

P. SAUVAN[1], A. YA. FAENOV[2,3], E. DALIMIER[4], E. OKS[5], T. A. PIKUZ[2,3] AND I. YU. SKOBELEV[2]

[1]*Departamento de Ingeniería Energética, ETS Ingenieros Industriales, UNED, C/Juan del Rosal 12,28040 Madrid, Spain*
[2]*Joint Institute for High Temperatures of Russian Academy of Sciences, Moscow, Russia*
[3]*Quantum Beam Science Directorate, Japan Atomic Energy Agency, 8-1 Umemidai Kizugawa, Kyoto 619-0215, Japan*
[4]*Laboratoire pour l'Utilisation des Lasers Intenses UMR 7605, CNRS-CEA-Ecole Polytechnique-Université Paris 6, case 128, 4 Place Jussieu, 75252 Paris Cedex 05 and 91128 Palaiseau, France*
[5]*Physics Department, 206 Allison Laboratory, Auburn University, Auburn, AL 36849, USA*

ABSTRACT: We analyze features in spectral line profiles of F IX L_α and F VIII He_β under a strong Quasi-monochromatic Electric Field (QEF) caused by the interaction of a plasma with a strong laser field. The experiment was performed at the Ti:Sa laser facility at Polytechnico di Milano. The experimental profiles exhibit prominent modulations. We identified the modulations as the satellites caused by the QEF in the plasma. In our analysis we took into account the following: (1) Stark broadening by the ion and electron microfields; (2) Doppler broadening; (3) opacity; (4) effects of the laser field calculated using the Floquet-Liouville formalism; (5) a time evolution of the laser pulse. We demonstrated that the primary factor in explaining the experimental line profiles is the satellites caused by the QEF. In the present experiment, the width of the satellites was comparable with the separation between them. Therefore, it was also possible to analyze the experimental profiles in terms of a "broadening" by the QEF. We also showed that the Doppler broadening plays an important role in simulating the line profiles observed in the present experiment.

PACS: 52.38.-r, 32.70.-n, 52.70.-m, 32.60.+i

1. INTRODUCTION

In plasmas subjected to a very intensive laser field, profiles of spectral lines of multi-charged ions are significantly affected by a strong Quasi-monochromatic Electric Field (QEF). The QEF arises in a process of laser-plasma interaction. Several studies of the corresponding spectral signatures have been published in recent years. Paper [1] presented experimental and theoretical studies of F IX L_α line in the experiments conducted at the Neodim terawatt laser facility in Russia (the laser power density 3×10^{17} W cm^{-2}). Paper [2], where general principles of spectroscopic diagnostics of plasmas containing a QEF have been summarized, presented experimental and theoretical studies of Al XII β line (a.k.a. Al He_β) performed at the Jena laser system JETI – see also a later paper [3]. A common feature of these studies was an appearance of a complicated sequence of peaks and depressions in spectral line profiles. They have been caused primarily by the interplay of a QES and the ion microfield – the interplay that can manifest quite differently under various experimental conditions (see, e.g., book [4]).

In the current paper we present experimental and theoretical studies of F IX L_α line and of F VIII β line (a.k.a. F VIII He_β) in the experiments conducted at the Ti:Sa laser facility at Polytechnico di Milano.

2. EXPERIMENTAL SETUP AND SPECTRA PROCESSING

The experiment has been performed using a Ti: Sapphire (Ti: Sa) laser system of National Laboratory for Ultrafast and Ultraintense Optical Science (ULTRAS-CNR-INFM, Politecnico di Milano, Italy), which generates 800 nm pulses with 10 Hz repetition rate, maximum energy of 128 mJ, and laser pulse duration of 300 and 600 fs. The laser pulse contrast was $\sim 10^{-5}$ in the nanosecond time scale and $\sim 10^{-4}$ in the ps scale [5 – 9].

A teflon slab (CF_2) was used as the target in the present experiment. The laser beam was focused on a target surface at the incidence angle 15° by an off-axis parabola mirror in a spot of ~ 20 µm in diameter. The laser power density for 128 mJ energy of the pulse varied in the range $Q_{las} = (0.5 - 1.0) \times 10^{17}$ W cm^{-2} for the used laser pulse durations. The target was continuously shifted in order to shot each time on a fresh surface.

X-ray radiation spectra of plasma were measured [8] by the focusing spectrometer with spatial resolution (FSSR) based on the spherically bent mica crystal ($2d$ = 1.991 nm). The x-ray radiation was registered by the CCD camera (Roper Scientific, 1300×1300-cells matrix) with the cell size of 20 µm. The CCD-matrix was protected from the visible and VUV radiation by three layers of the 1-µm polypropylene film covered by the 0.2-µm aluminum layer.

Such configuration enabled us to observe the He_β line of He-like ion F VIII (1s3p – 1s^2 resonance transition) and the Ly_α line in H-like ion F IX (2p – 1s resonance transition) with the spectral resolution $\lambda / \Delta\lambda \approx 5000$ in the wavelength range 1.41 – 1.62 nm. The spectral measurements were performed with the one-dimensional spatial resolution about 50 µm transverse to the plasma expansion direction.

To reduce the noise CCD data was read-out each 2 sec, which corresponds to 20 shots on the target. This is why we always operated with already averaged data. The laser, the target motion and the CCD camera were controlled by Lab-View routine. Sorted and numbered spectra were saved automatically to ASCII files, thus simplifying further data processing. MatLab software was used for processing of collected spectra. Typically the signal occupies four-five columns of CCD matrix due to the special resolution of the spectrograph. To extract a useful information from rather noisy spectra generated by high laser intensity pulses, it was necessary to remove the noise from them. The noise had a form of spikes and arose when various high energy particles struck the CCD detector surface. This is why, to obtain spectra with a suitable level of noise, a series of eight-ten spectra were processed by spikes removal algorithm (M2M [8,10]). Since laser beam fluctuations strongly affect the line shape and the intensity, we always tried to choose those spectra that were very similar. If there were spectra in the cleaned series that differ greatly from others, they were replaced by new spectra until all eight spectra had almost the same shape and the intensity level.

X-Ray spectra observed for various values of the laser power density are shown in Fig. 1. These spectra contain He_β line of F VIII ion and Ly_α line of F IX ion.

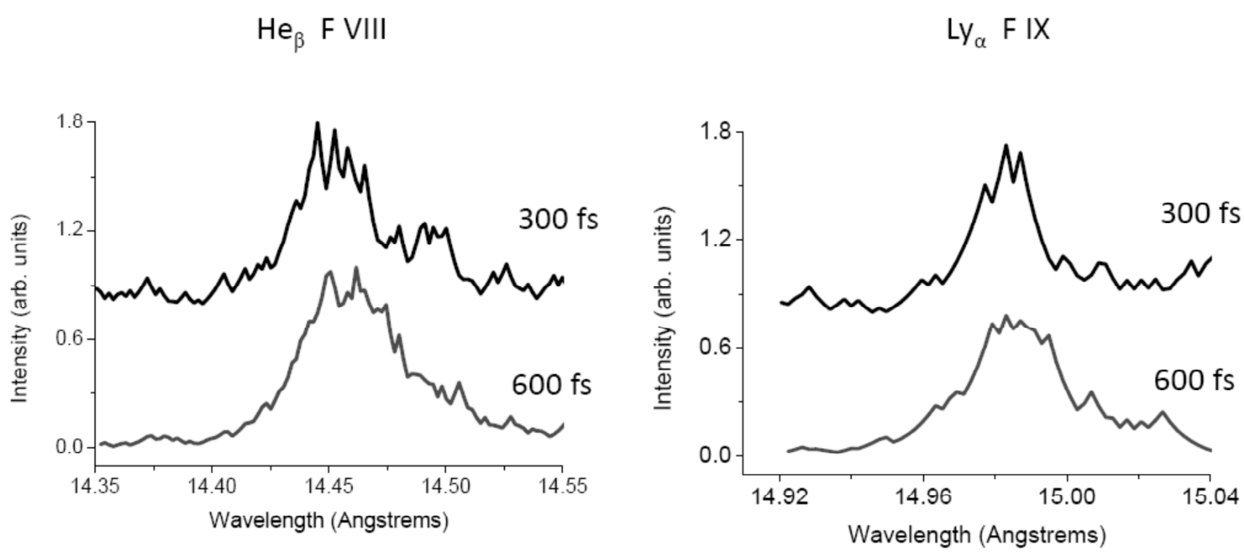

Figure 1: X-Ray spectra observed for various values of the laser pulse duration.

3. ANALYTICAL ESTIMATES

We use analytical estimates to identify the expected primary spectral manifestation of the electric fields involved, and to verify the result by comparing with the experimental spectra. This can be done in the simplest way for hydrogenic spectral lines.

The relation between the amplitude E_0 of the QEF in the plasma and the characteristic strength F_i of the quasistatic part of the ion microfield determines two very different theoretical scenarios – in accordance to book [4].

In the case where $E_0 < F_i$, there is an interplay of the two fields. As a result, one could expect observing so-called dips (or depressions) in the line profile at the distances from the line center proportional to $\lambda_0^2\omega/(2\pi c)$, where λ_0 is the unperturbed wavelength of the line, ω is the QEF frequency, and c is the speed of light. The proportionality coefficients are (in the first approximation) rational numbers such as $(nq - n_0q_0) / n$ and $(nq - n_0q_0) / n_0$, where n and n_0 are the principal quantum numbers of the upper and lower levels, respectively, while q and q_0 are the electric quantum numbers of the upper and lower levels, respectively.

In the opposite case where $E_0 >> F_i$, the quasistatic part of the ion microfield practically does not play any role. It would be expected observing one or several satellites at the distances from the line center equal to $\pm k \lambda_0^2\omega/(2\pi c)$, where $k = 1, 2, 3, \ldots$, or a "broadening" by the QEF. The broadening by the QEF would occur, if the width of the satellites profiles (caused by other broadening mechanisms) would exceed the separation between the satellites.

At the laser power density used in the present experiment, the QEF in the plasma can be expected to have the amplitude $E_0 \sim 10^{10}$ V/cm – in accordance to the formula E_0 (V/cm) = $[240\pi\ P(W/cm^2)]^{1/2}$. As for the quasistatic part of the ion microfield, its characteristic strength F_i, can be estimated by the formula F_i(V/cm) ~ $10^{-6}Z_p^{1/3}[N_e(cm^{-3})]^{2/3}$, where Z_p is the charge of perturbing ions and N_e is the electron density. For $Z_p = 9$ and $N_e = 10^{20}$ cm^{-3}, we obtain $F_i \sim 5x10^7$ V/cm.

Thus, we deal with the case where one could observe either individual satellites or a broadening by the QEF. The expected number of the satellites in each wing of hydrogenic line is given by formula (3.1.11) of book [4]:

$$p_1(X\varepsilon) = X\varepsilon - 0.809(X\varepsilon)^{1/3} \tag{1}$$

(it is understood that the number of the satellites in each wing can be obtained by rounding up the value of p_1 to the closest integer). Here

$$X = (nq - n_0q_0) / Z_r, \tag{2}$$

where Z_r is the nuclear charge of the radiating ion. The quantity ε is the modulation parameter defined as follows

$$\varepsilon = 3\hbar E_0/(2m_e e\omega), \tag{3}$$

where $\hbar$ is the Plank constant. Substituting in Eqs. (1), (3) $X = 2/9$ (for the line F IX L_α), $\omega = 2.354x10^{15}$ s^{-1} (corresponding to $\hbar\omega = 1.549$ eV), $E_0 = 2.7x10^9$ V/cm = $9x10^6$ CGSE (corresponding to the QEF power density 10^{16} W/cm^2), we find $p_1 = 1.9$. Thus, the theory from book [4] predicts two satellites in each wing of the line F IX L_α. This prediction is in excellent agreement with the experiment, as well as with simulations presented below.

In the present experiment, the width of the satellites is comparable with the separation between them. Therefore, it is also possible to analyze the experimental profiles in terms of a "broadening" by the QEF. For the line F IX L_α, the broadening by the QEF predominantly affects the lateral components of the line. Since for this line, each of the two lateral components is 4 times less intense than the central components, the broadening by the QEF would lead to the appearance of a broad "pedestal" superimposed with a narrower central component. The Full Width at Half Maximum (FWHM) of the pedestal $\Delta\lambda_{1/2}$ can be estimated as follows:

$$\Delta\lambda_{1/2} = [\lambda_0^2\omega / (\pi c)]p_1(X\varepsilon). \tag{4}$$

Substituting the same parameters as those used above for estimating the value of p_1, we find the expected FWHM of the pedestal:

$$\Delta\lambda_{1/2} = 0.1 \text{ A}. \tag{5}$$

This analytical result is in a good agreement with the experimental profile.

4. SIMULATIONS

For incorporating effects of the QEF in the plasma, we used a so-called Floquet-Liouville formalism [11]. The Floquet-Liouville operator, introduced to solve the time-dependent problem (Stark effect in a time-dependent QEF), leads to a time-independent treatment carried out via an operator of the infinite dimension. Nevertheless, the periodic property of this operator allows one to consider only the projection of the Floquet-Liouville operator on the Floquet subspace of the fixed principal quantum number n. Depending on the coupling between the Floquet subspaces for the Floquet-Liouville operator, for any desired accuracy of the line shape calculation, there exists a value of n, at which the Floquet subspace can be truncated.

More specifically, in the simulations we accounted for the contribution of the different amplitudes of the QEF during the laser pulse using the formula:

$$I_\lambda = \int_{-t_o}^{t_0} \varepsilon_{line}(t)\varphi_\lambda(E(t))dt \qquad (6)$$

Here $\varphi_\lambda(E(t))$ is the line profile depending on the QEF $E(t)$ and $\varepsilon_{line}(t)$ the line emissivity during the laser pulse. Further, we assumed that all contributions radiated with the same intensity $\varepsilon_{line} = 1$.

We considered a Gaussian shape of the laser pulse. We allowed also for the Doppler broadening. It was the next most important broadening mechanism due to the fact that the ion temperature T_i is much greater than the electron temperature T_e – by about two orders of magnitude. A self-absorption has been taken into account in accordance to the formula

$$S_\lambda = (1 - \exp(-kI_\lambda)), \qquad (7)$$

where k is an adjustable parameter.

The plasma parameters have been chosen as follows: $N_e = 10^{20}$ cm^{-3}, Te = 100 eV. It should be emphasized that the simulated profiles are not sensitive to these values because the Stark broadening by ion and electron microfields is much smaller than the broadening mechanisms discussed above.

The best fit to the experimental profiles is shown in Figs. 2 and 3. The ion temperature used in the simulations is displayed in each Figure.

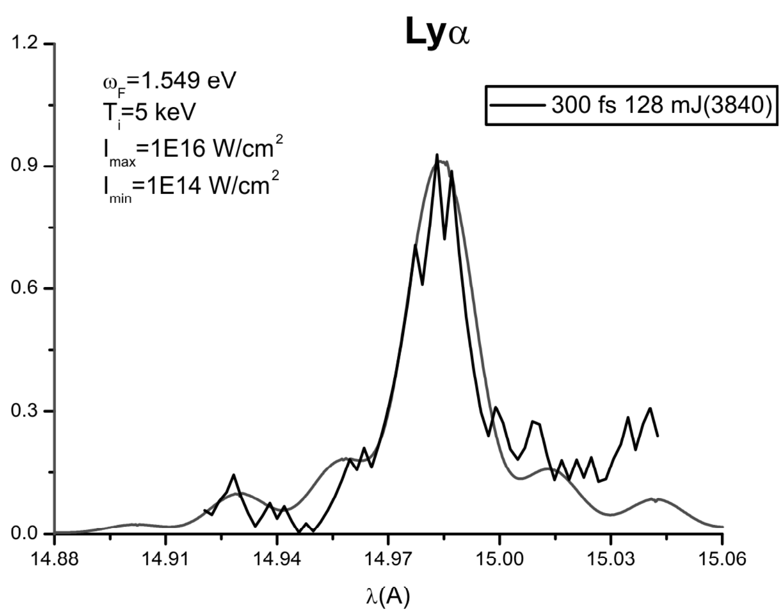

Figure 2: Experimental Profile and the Simulated Profile (Smooth Curve) of the Line F IX L_α

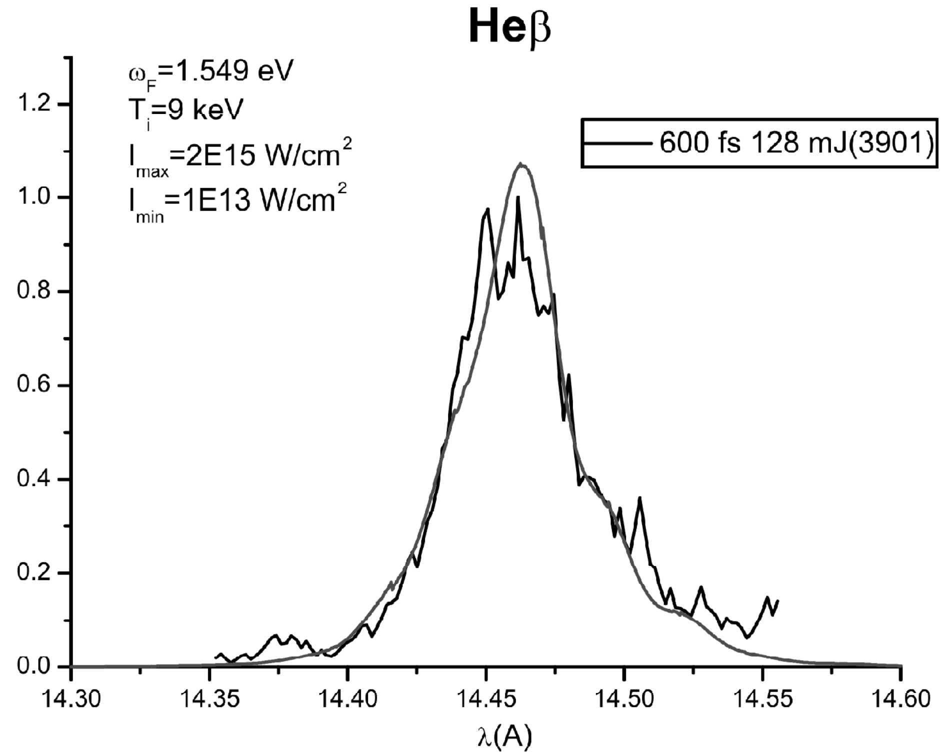

Figure 3: Experimental Profile and the Simulated Profile (Smooth Curve) of the Line F VIII He$_{\alpha}$

5. CONCLUSIONS

We demonstrated that the primary factor in explaining the experimental line profiles is the satellites and/or the "broadening" caused by the QEF. The broadening by the QEF occurs when the width of the satellites profiles (caused by other broadening mechanisms) exceeds the separation between the satellites. To the best of our knowledge, this has never been previously discussed in relation to previously published experimental line profiles.

We also showed that the Doppler broadening plays an important role in simulating the line profiles observed in the present experiment. This is because the ion temperature T_i was much greater than the electron temperature T_e – by about two orders of magnitude.

The experimental profiles exhibit a red asymmetry. All possible causes of the asymmetry have not been incorporated in the simulations yet. For the line *F* IX L$_{\alpha}$, the primary cause of the asymmetry is probably the anomalous velocity distribution of plasma ions. However, in order to draw the anomalous velocity distribution from the observed asymmetry, it is necessary to take into account other sources of the asymmetry: the latter must be subtracted from the observed asymmetry before trying to deduce the information on the anomalous velocity distribution.

A preliminary analysis shows that among the other sources of the asymmetry, one of the most significant could be a so-called trivial asymmetry. The trivial asymmetry arises due to a peculiar relation between the spectral line profile $I(\omega)$ in the frequency scale and the corresponding spectral line profile $S(\lambda)$ in the wavelength scale: $S(\lambda) = (2\pi c / \lambda^2)\, I(2\pi c / \lambda)$. Even if the profile in the frequency scale $I(\omega)$ is symmetric, the corresponding profile in the wavelength scale $S(\lambda)$ exhibits a red asymmetry (see, e.g., [12]). We emphasize that the greater is the width of the line, the further in the red wing should be seen the effect of the trivial asymmetry. Our estimate shows that in the present experiment, the trivial asymmetry contribution should be important at the distance ~ 0.05 A in the red wing – just where it is most prominently observed.

For the line F VIII He$_{\beta}$, another possible source of the red asymmetry can be the asymmetric theoretical positions of the satellites.

A more detailed discussion of the observed red asymmetry and the incorporation of its causes into simulations will be published elsewhere.

Acknowledgements

This work was partly supported by the Russian Foundation for Basic Research 10-02-00345-a and 12-02-91169-GFEN-a, as well as by the RAS Presidium Program of fundamental research No. 2.

References

[1] V. S. Belyaev, V. I. Vinogradov, A. S. Kurilov, A. P. Matafonov, V. S. Lisitsa, V. P. Gavrilenko, A.Ya. Faenov, T.A. Pikuz, I. Yu. Skobelev, A. I. Magunov, and S.A. Pikuz, Jr., *JETP* **99**, 708, (2004).

[2] P. Sauvan, E. Dalimier, E. Oks, O. Renner, S. Weber, C. Riconda, *J. Phys. B: At. Mol. Opt. Phys.* **42**, 1950001, (2009).

[3] P. Sauvan, E. Dalimier, E. Oks, O. Renner, S. Weber, C. Riconda, *Intern. Review of Atom. and Molec. Phys.* **1**, 123, (2010).

[4] E. Oks, *Plasma Spectroscopy: The Influence of Microwave and Laser Fields*, Springer Series on Atoms and Plasmas, Vol. 9 (Springer, Berlin) 1995.

[5] F. Calegari, S. Stagira, C. D'Andrea, G. Valentini, C. Vozzi, M. Nisoly, S. De Silvestri, L. Poletto, P. Villoresi, A. Faenov, T. Pikuz, Appl. Phys. Lett. **89**, 111122, (2006).

[6] A. Ya. Faenov, A. I Magunov, T.A. Pikuz, I Yu. Skobelev, S. V. Gasilov, S. Stagira, F. Calegari, M. Nisoli, S. De Silvestri, L. Poletto, P. Villoresi, and A.A. Andreev, *JETP Lett.* **84**, 308, (2006).

[7] A. Ya. Faenov, A. I. Magunov, T. A. Pikuz, I. Yu. Skobelev, S. Stagira, F. Calegari, M. Nisoli, S. De Silvestri, L. Poletto, P. Villoresi, and A.A. Andreev, Laser Particle Beams **25**, 267, (2007).

[8] A. Ya. Faenov, V. P. Gavrilenko, A. I. Magunov, T. A. Pikuz, I.Yu. Skobelev, S. V. Gasilov, S. Stagira, F. Calegari, C. Vozzi, M. Nisoli, G. Sansone, S.De Silvestri, L. Poletto, and P. Villoresi, *AIP Conference Proceedings* (Melville, New York) **1024**, 242 (2008).

[9] N. D. Ouart, A. S. Safronova, A. Ya. Faenov, T.A. Pikuz, S. V. Gasilov, F. Calegari, M. Nisoli, S. De Silvestri, S. Stagira, L. Poletto, P. Villoresi, *J. Phys. B: At. Mol. Opt. Phys.* **44**, 065602, (2011).

[10] S.V. Gasilov, A. Ya. Faenov, T. A. Pikuz, P. Villoresi, L. Poletto, S. Stagira, F. Calegari, C. Vozzi, M. Nisoli, *J. App. Phys.* **102**, 063303, (2007).

[11] P. Sauvan and E. Dalimier, Phys. Rev. E **79**, 036405, (2009).

[12] A.V. Demura, G. V. Demchenko, and D. Nikolic, *Eur. Phys. J. D* **46**, 111, (2008).